Influence of Operational Parameters and Kinetic Modelling of Catalytic Wet Air Oxidation of Phenol by Al/Zr Pillared Clay Catalyst

John, Moma*[+]***; Jeffrey, Baloyi***[•]

Molecular Sciences Institute, School of Chemistry, University of the Witwatersrand, P/Bag 3, WITS 2050, Johannesburg, SOUTH AFRICA

Thabang, Ntho

Advanced Materials Division, MINTEK, Private Bag X3015, Randburg 2125, SOUTH AFRICA

ABSTRACT: *Single and mixed oxide Al/Zr-pillared clay (Al/Zr-PILC) catalysts were synthesized and tested for catalytic wet air oxidation (CWAO) of aqueous phenol solution under milder conditions, in a semi-batch reactor. The catalysts were synthesized from natural bentonite clay using ultrasonic treatment during the aging and intercalation steps and were characterized using High Resolution Scanning Electron Microscopy-Energy Dispersive angle X-ray spectrometry (HRSEM-EDX), powder X-Ray Diffraction (p-XRD), nitrogen adsorption/desorption, Fourier Transforms InfraRed (FT-IR) spectroscopy and zeta potential. Successful pillaring of aluminum and zirconium oxides into the clay was confirmed by p-XRD with increased basal spacing (1.92 nm) and higher specific surface area (230 m^2/g). The influence of stirrer speed (200-1000 rpm), catalyst dosage (1-3 g/L), initial pH (1-3), initial phenol concentration (500-1500 mg/L), the effect of temperature (80-150 °C) and oxygen pressure (5-15 bar) was evaluated on phenol conversion and their reaction kinetics. At the optimum conditions of initial pH of 3, catalyst dosage of 2 g/L, initial phenol concentration of 1000 mg/L, reaction temperature of 100 °C and oxygen pressure of 10 bar, the complete removal of phenol was achieved by Al/Zr-PILC within 120 min. The CWAO process was well-described by the first-order power rate law kinetics model. The apparent activation energy of the reaction calculated by Arrhenius equation was 21.306 kJ/mol.*

KEYWORDS: *Kinetic modeling; Al/Zr pillared clay; phenol removal; catalytic wet air oxidation.*

INTRODUCTION

Wastewater containing phenol represent a threat to human beings and aquatic life, being regenerated by industrial processes such as petrochemicals, pharmaceuticals, resin manufacturing and refineries in the range of 200-1500 mg/L [1, 2]. Since phenol is stable, refractory, non-biodegradable, toxic to the living organism at very low

** To whom correspondence should be addressed.*

+ E-mail: john.moma@wits.ac.za

• Other Address: Advanced Materials Division, MINTEK, Private Bag X3015, Randburg 2125, SOUTH AFRICA

1021-9986/2019/6/189-203 15/$/6.05

concentration and poisonous to soil microbes, their discharge into the environment without treatment poses severe environmental and health problems. Given these reasons, the treatment of phenol wastewater is important before being released into the environment. Advanced Oxidation Processes (AOPs) specifically Catalytic Wet Air Oxidation (CWAO), appears as one of the preferred feasible and effective methods for the removal of non-biodegradable refractory organic compounds such as phenol [3]. In general, CWAO is a liquid phase oxidation process in which oxygen or air is used to oxidize refractory organic compounds into carbon dioxide and water in the presence of suitable solid catalyst, without any toxic gaseous emission. CWAO process can be operated at mild temperature and pressure conditions, which are very attractive process economics. Unfortunately, the lack of stable and active catalysts, which results in high capital investment and high operating costs limits the large-scale application of CWAO.

Noble metal supported catalysts have been reported to be active for the CWAO treatment of refractory organic contaminants, however, the main disadvantage for these catalysts are costs, deactivation, sintering, leaching and deposition of carbonaceous material on the catalysts surface [4, 5]. The use of Pillared Interlayered Clays (PILC) as heterogeneous catalysts in CWAO has been proposed due to their excellent physiochemical, abundant, low cost, simplicity of the pillaring process and catalytic properties. However, traditional process for synthesis of PILC involves prolonged times (1-5 days) and large amount of water (2 wt. % suspension), and such requirements significantly hinder the scale-up of the pillaring process to industrial scale [6, 7]. Many strategies such as use of concentrated clay suspension, dry clay, addition of dry clay to pillaring solutions have been proposed as ways of overcoming the above-mentioned problems. Microwave irradiation and ultrasonic treatment during the synthesis of PILC, in which the aging and ion exchange processes occur within minutes (5-30 minutes) has also been reported. The use of mixed metal oxides for the pillaring of the clay has been found to improve properties of PILC compared to single metal oxide [7, 8]. However, CWAO process using PILC heterogeneous catalysts is not only influenced by origin and features of the catalysts but also the operational parameters used. Therefore, in order to determine the feasibility of CWAO for practical use, it is crucial to investigate influence of operational parameters on the efficiency of CWAO on the removal of refractory organic pollutants.

In this context, the objective of this study is to synthesize single and mixed Al/Zr-PILC catalysts from South African natural bentonite clay using ultrasonic treatment during the pillaring and intercalation steps and test them as heterogeneous catalysts for CWAO of phenol. The influence of several significant operation parameters such as stirrer speed, catalyst dosage, initial pH, initial phenol concentration, reaction temperature and oxygen pressure on the CWAO of phenol have also been studied in detail.

EXPERIMENTAL SECTION

Catalyst synthesis

The starting material was natural clay from deposit of Cape Town bentonite mine (Western Cape Province, South Africa). The Cation Exchange Capacity (CEC) of natural clay was 78.6 meq/g. The natural clay was used as received without further purification. The pillaring agent solution was prepared by the slow addition of a NaOH solution (0.4 M, 500 mL) into a 250 mL of 0.4 M $Al(NO_3)_3{\cdot}9H_2O$ or $Zr(NO_3)_4.5H_2O$ at room temperature under vigorous stirring for 120 min until an $[OH^-]/[Al^{3+}$ or Zr^{4+} or $Al^{3+} + Zr^{4+}]$ molar ratio of 2:1 was achieved. The solution was then ultrasonicated for 10 min at 25 °C. The resulting pillaring agent solution was then added directly into dry bentonite clay, at ratio of 3.33 mmol of (Al + Zr)/g sodium bentonite (25 mL pillaring solution/1 g) and stirred at 25 °C for 30 min. The resulting dispersion was ultrasonicated for 10 min at room temperature to perform ion exchange, followed by filtering, washing with high purity water (5 times with 200 mL portions) and centrifuged at 4000 rpm for 8 min. The obtained solids were oven-dried overnight at 120 °C and calcined at 500 °C for 120 min in a muffle furnace.

Characterization of the catalysts

High resolution scanning electron microscopy (HRTEM) was performed on a FEI Nova NanoSem 200 from FEI Company. The elemental analysis was performed by EDX which was equipped to HRSEM. Powder X-ray diffractograms (p-XRD) were recorded on a high resolution Bruker AXS D8 X-ray advanced

powder diffractometer using CoKα-radiation (40 kV, 40 mA, 1.78897 Å) and scanning in the range of 2θ over 5 to 80° at scanning speed of 0.02˚/s. Brunauer−Emmett−Teller (BET) specific surface areas, average pore diameters, pore volumes and Barrett-Joiner-Halenda (BJH) pore size distribution of the catalyst samples were determined by N_2 adsorption/desorption at −196 °C using a Micrometrics ASAP Tristar 3000 unit. The samples were place in the sample holder and degassed in a vacuum at 150 °C for 4 h before analysis. FTIR spectroscopic measurements were performed on a Varian 640-IR FTIR spectrometer with a Miracle single bounce diamond ATR cell from PIKE Technologies. Zeta potential was determined by Zetasizer Nano ZS (Malvern Instruments, UK) and the Cation Exchange Capacity (CEC) was obtained using Kjeldhal technique.

Catalytic oxidation of phenol solutions

The CWAO experiments were carried out in a 350 mL high-pressure autoclave "semi-batch type" reactor (Parr model 4531M) equipped with a magnetic stirrer to eliminate mass transfer limitations of oxygen from the gas to liquid phase. The reactor was fitted with a removable glass lining and loaded with 250 mL of aqueous phenol solution (500-1500 mg/L) at desired initial pH over the range of 3-4 and a desired amount of a catalyst (1-3 g/L). After reaching the adsorption/ desorption equilibrium, the reaction mixture inside the reactor was purged with N_2 and then heated to the desired temperature between 80 to 150 °C. Once the desired temperature was reached, pure oxygen pressure (5-15 bar) was introduced into the reactor and a first sample was withdrawn for analysis in which it was set as "zero time". Thereafter, liquid samples were withdrawn at regular time intervals by a syringe and immediately filtered by 0.45 μm pore size nylon micro filter into a HPLC vial. All experiments were conducted in triplicate and the average data used. The concentrations of phenol were analyzed with an HPLC system (LC-10AD, Shimadzu, Kyoto, Japan) using an ODS-3 column and UV detector at a detection wavelength of 254 nm. The mobile phase was a mixture of methanol and water (60:40, v/v) slightly acidified with 0.1% acetic acid at a flow rate of 1 mL/min and 20 μL injection volume. The evolution of phenol intermediates during the reaction were analysed by HPLC following the method described by *Ma et al.* [9]. Total organic carbon (TOC) was measured to determine the mineralization degree of phenol by a Shimadzu TOC analyzer.

Kinetic study

The CWAO reaction kinetics for the phenol oxidation reaction is required to provide complete interpretation of the data obtained in the semi-batch reactor. Many researchers [2, 3, 10, 11] in the literature have described the oxidation rates of phenol oxidation using a simple power law expression. All experimental data were fitted to a power rate law and represented by the following equation:

$$r_a = -\frac{dC_{ph}}{dt} k_1 C_{O_2} C_{ph}^a \quad (1)$$

Where r_a is the rate of phenol oxidation reaction; α is the reaction order with respect to phenol; Co_2 is the oxygen concentration; k_1 is the intrinsic reaction rate constant. Assuming a constant concentration of oxygen, the power rate law becomes

$$-\frac{dC_{ph}}{dt} k_{ap} C_{ph}^a \quad (2)$$

The majority of authors previously reported that the CWAO of pure phenol oxidation reaction follows first-order kinetics with respect to the phenol concentration [2, 3, 12-16]. Assuming a first order reaction with respect to phenol concentration, Equation 2 can be integrated for α = 1 to become:

$$-\ln C_{ph} = k_{ap} t + \times \quad (3)$$

$$-\ln\left(\frac{C_{ph}}{C_{0\,ph}}\right) = k_{ap} t \quad (4)$$

Where k_{at} (min^{-1}) is the apparent first-order kinetic rate constant, which can be determined from the slope of $-\ln\left(\frac{C_{ph}}{C_{0\,ph}}\right)$ versus *t*, C_{ph} and $C_{0\ ph}$ represent both the final and initial concentration of phenol, respectively.

Activation energy

Assuming an Arrhenius dependence of temperature, apparent activation energy of phenol conversion can be expressed as follows

$$k_{ap} = k_0 \exp\left[-\frac{E_a}{RT}\right] \quad (5)$$

Eq. (5) can be written in the logarithmic form:

$$\ln k_{ap} = \ln k_0 - \frac{E_a}{RT} \quad (6)$$

Where E_a is apparent activation energy (kJ/mol); k_o is pre-exponential factor (min^{-1}); k_{ap} is apparent reaction rate constant (min^{-1}); T is the reaction temperature (K); R is the universal gas constant (8.314 J/mol K).

RESULTS AND DISCUSSION

Catalysts characterization

The chemical composition of natural clay and pillared clay catalysts, as determined by EDS, are reported in Table 1S in the supplementary materials. The chemical weight composition of natural clay confirms SiO_2 and Al_2O_3 as the major constituents of the natural clay with other mineral oxides impurities such as Na_2O, CaO, MgO, K_2O and Fe_2O_3. The high content of Si and Al oxides revealed the existence of quartz and muscovite, whereas the high content oxides of Na compared to Ca confirmed that the natural bentonite is in the sodium form (Na^+) [17, 18]. After the pillaring process the aluminium and zirconium oxides content in the pillared clay catalysts increased from 15.31 to 31.98 wt% and from 0 to 38.19 wt% respectively. The SEM micrographs of natural clay and pillared clay are presented in Fig. 2. The morphology of natural and pillared bentonite clay have tightly packed patterns with porous and rough surface. There are no observable differences in the morphology of the surface of natural and pillared bentonite clays. It is noteworthy that the natural bentonite clay structure was still intact after pillaring process, thus, indicating that the mechanical structure of natural bentonite clay was not affected by the pillaring process.

The surface area, total pore volume, micropore volume and pore diameter of natural and pillared bentonite clays are shown in Table 2S. The expansion of natural bentonite clay structure and desegregation of the bentonite clay particles during the pillaring process leads to a significant increase of the specific surface area and porosity in the pillared bentonite clay catalysts. The increase in the specific surface area and porosity for the single metal oxides (Al or Zr) pillared bentonite clay samples were lower compared to mixed metal oxides (Al/Zr) pillared catalysts. The specific surface area and the micropore volume of natural bentonite clay increased from 61 to 230 m^2/g and 0.089 to 0.115 cm^3/g respectively with the high increase in the surface area for pillared bentonite clay indicating successful pillaring of Al and Zr metal oxides species into the silicate layers of the bentonite clay. These results are in agreement with previous reports by different researchers [8, 19-23].

To study the nature of the change of charge on the surface of materials, their zeta potentials were measured. The zeta potential values of natural clay and pillared bentonite clay at different pH values are shown in Fig. 2. The point of zero charge for different samples was determined by plotting the zeta potential values of the suspension as function of pH values [24]. As can be seen, the natural bentonite clay has negative zeta potential values in the pH range of 1 to 10. The high permanent negative charge on the basal surface of Na-Bt clay particles might arise from high degree of isomorphous substitution of structural Si^{4+} in the tetrahedral layer by Fe^{3+} or Al^{3+} while Al^{3+} in the octahedral layer is substituted by Fe^{2+} or Mg^{2+} [25] as well as the pH independent charge arising from the hydroxyl groups at the edges of the natural bentonite clay particles. The decrease in negative zeta potential from 27 to 17.5 mV with increasing pH values (H^+ ions) in the solution can be attributed to this pH independent charge. In contrast, the pillared bentonite clays have higher zeta potentials than natural bentonite clay, which reflect that positive charges have been introduced into natural bentonite clay during the intercalation process resulting in less negatively charged pillared bentonite clays. This might be attributed to the formed oxide pillars between Na-Bt layers due to the hydration of zirconium or aluminium polycations intercalated into the interlamellar space upon calcination.

XRD patterns of both the natural and pillared bentonite clays are shown in Fig. 3. The XRD data confirms that the natural bentonite clay contains Na-montmorillonite with other impurities such as quartz, muscovite and calcite. A shift of the signal related to (001) sodium montmorillonite planes at $2\theta = 8.8^\circ$ to $2\theta = 7.3 - 6.88^\circ$ was observed. The basal *d*-spacing (d_{001}) and 2 theta angle values for materials are listed in Table 3S in the supplementary material. The basal *d*-spacing (d_{001}) increased from 1.56 nm in the natural bentonite to

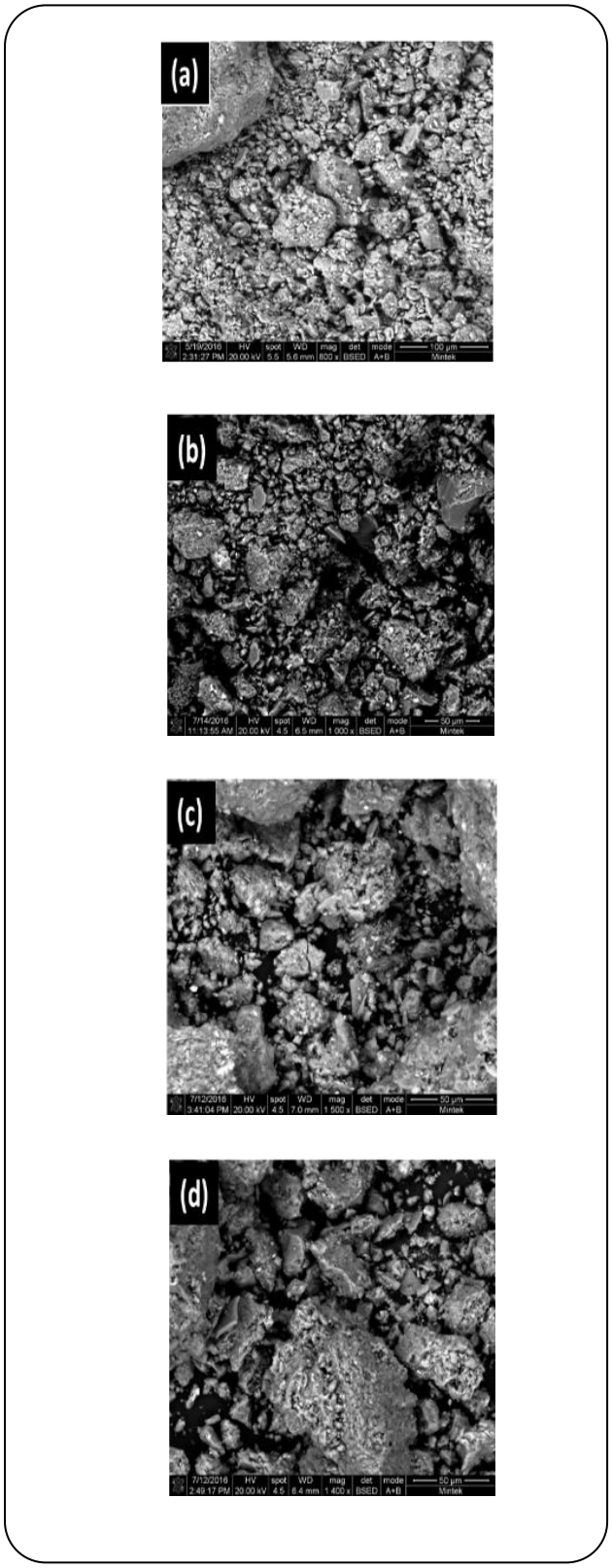

Fig. 1: HRSEM micrographs of (a) Na-Bt, (b) Al-PILC, (c) Zr-PILC and (d) Al/Zr-PILC (3:1).

1.72-1.92 nm in the pillared bentonite clay due to pillaring process. This shift is expected due to expansion of the interlayer space of the natural bentonite clay after pillaring process, thus, indicating a successful intercalation of active metal oxides clusters (Al, Zr or Al/Zr) into silicate layers.

FTIR spectroscopy further confirmed the effectiveness of the pillaring process. The FTIR spectra (400 – 4000 cm^{-1}) of both the natural and pillared bentonite clay materials are shown in Fig. 4. The FT-IR spectrum of the natural bentonite clay exhibits two peaks at 3583 and 3294 cm^{-1} in the –OH stretching region. These two peaks correspond to –OH stretching vibrations of structural hydroxyl groups in the bentonite clay and water molecules (H-bonded water) present in the interlayer [26-28]. After pillaring, these peaks at 3583 and 3294 cm^{-1} appeared broadened and their intensity decreased due to the existence of Keggin-OH and Keggin-H_2O stretches and hydration of interlayer water molecules, respectively [29, 30]. The peak near 1630 cm^{-1} corresponds to H-O-H bending vibration of water, while the peak at approximately 978 cm^{-1} corresponds to the siloxane (Si-O-Si) group stretching vibration in the tetrahedral structure of the bentonite clay [27, 31], but the peak shifted to higher wavelength (978 to 1088 cm^{-1}) due to pillaring in all the pillared materials. The peaks at 906 and 771 cm^{-1} can be assigned to Al-OH and MgO-H stretching vibrations, respectively [27]. The peaks resulting from Si-O bending and Al-O stretching vibration are observed at 561 and 611 cm^{-1} respectively [6].

Pyridine has been used as a probe molecule to study the chemical nature of acidic sites in the natural and pillared bentonite clay samples [8, 21,]. As shown in Fig. 5 the FT-IR spectra of adsorbed pyridine base molecule in the region of 1650 -1400 cm^{-1} were utilized to discriminate the Lewis and Brönsted acid sites on the samples. Following the pyridine adsorption on natural and pillared bentonite samples, the peaks at 1443, 1491, 1522, 1541, 1558 and 1635 cm^{-1} were observed. The peaks at 1443 and 1541 cm^{-1} represent the pyridine molecules interacted with Brönsted (B) acid sites [8, 21] whereas the peaks at 1491, 1522 and 1635 cm^{-1} represent the pyridine molecules interacted with the Lewis acid site (L) [8, 32-34]. Moreover, the peak at 1558 cm^{-1} mainly corresponds to the pyridine species held by both the Brönsted and Lewis sites [8, 21, 32-34]. The presence

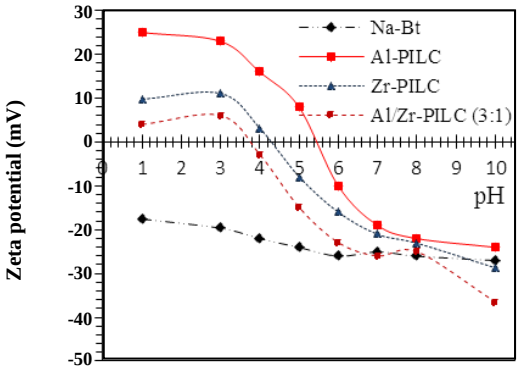

Fig. 2: Zeta potential (mV) values as a function of pH for natural and pillared bentonite clay.

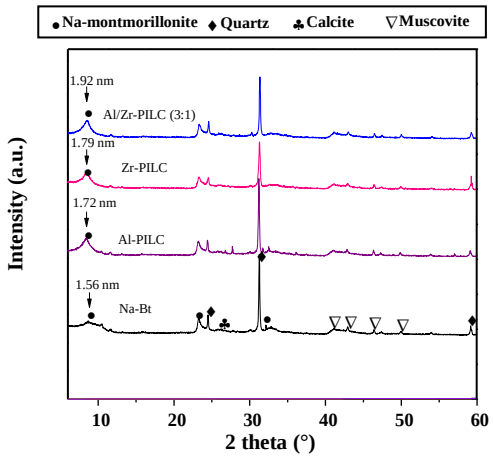

Fig. 3: XRD spectra of natural bentonite clay and pillared bentonite clay samples.

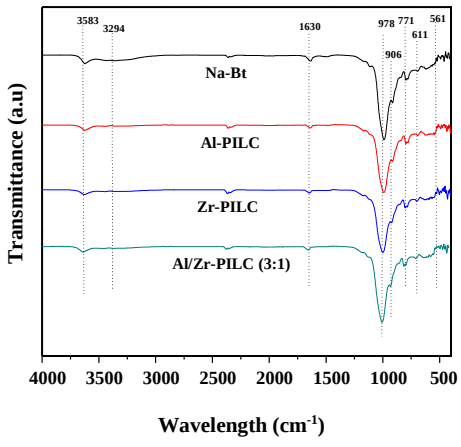

Fig. 4: FT-IR spectra of natural bentonite clay and different pillared bentonite clay samples.

of the Brönsted acid sites on the surface acidity of the pillared bentonite clay, is reported to be favorable for the phenol oxidation reaction [8, 31,].

CWAO of phenol and the evolution of intermediates

Fig. 6(a) shows the phenol conversion with reaction time over natural bentonite clay and pillared bentonite clay. A control experiment (without any catalysts) was carried and 9% of phenol removal was achieved after 120 min, while more than 74% of phenol removal was achieved in the presence of pillared clay catalysts. It can be concluded that the non-catalytic Wet Air Oxidation (WAO) of phenol was not active under these operating conditions. The adsorption experiment was also carried out to test the phenol removal due to adsorption over pillared clay catalysts and only 3% of phenol was removed. However, when using pillared bentonite clay as catalysts in the CWAO, removal of phenol increased significantly with increasing reaction time and the phenol removal were 74%, 88% and 100% after 120 min reaction for Al-PILC, Zr-PILC and Al/Zr-PILC (3:1), respectively. It can thus be concluded that the pillared clays are efficient catalysts in the CWAO of phenol. Fig. 5(b) indicate the TOC removal in the CWAO of phenol. The TOC removal in the phenol oxidation by adsorption and in the absence of a catalyst was negligible. In contrast, the removal of TOC was significantly increased, 49%, 61% and 88% being achieved in less than 180 min with Al-PILC, Zr-PILC and Al/Zr-PILC (3:1), respectively, under pillared bentonite clay.

The experiments on the evolution of the intermediates in the CWAO of phenol over the Al/Zr-PILCs (3:1) catalyst were conducted and the results are shown in Fig. 7. The analysis of the reaction products revealed the presence of the following main intermediates; hydroquinone, acetic acid, formic acid, malonic acid, oxalic acid and maleic acid. The refractory aromatic intermediates such as hydroquinone was identified by HPLC analysis at the beginning of the experiments, and all of them show maximum concentrations within 90 min reaction time. Therefore, the results suggest that these compounds are intermediates, which are further oxidized into short chain carboxylic acids. Moreover, catechol and benzoquinone were not detected in the reaction as reported in the literature [39-41]. This can be due to the fact that these aromatic intermediates get rapidly oxidized, while

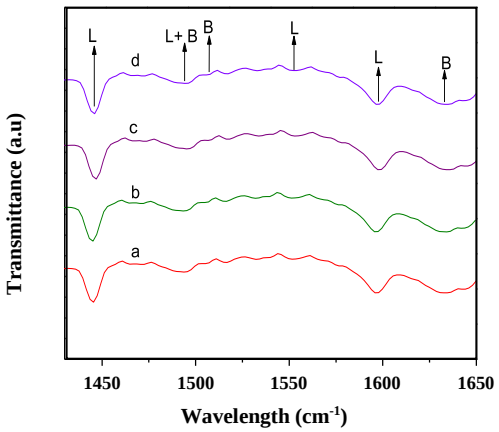

Fig. 5: FTIR spectra of the pyridine adsorbed of the bentonite samples (a) Bt, (b) Al-PILC, (c) Zr-PILC and (d) Al/Zr-PILC (3:1).

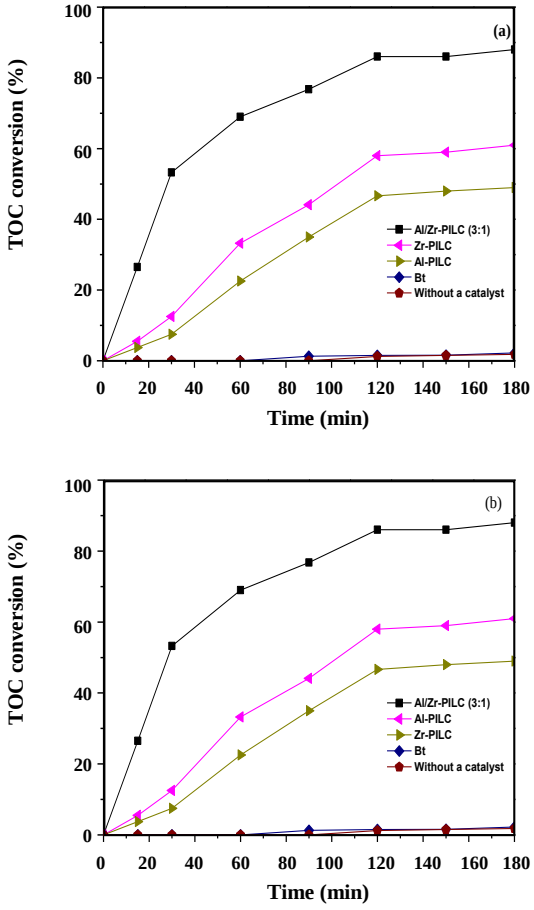

Fig. 6: CWAO of phenol over different catalysts (a) and TOC removal (b) under optimized experimental conditions (200 mL phenol solution, 1000 mg/L phenol concentration, 0.4 g of catalyst, 10 bar oxygen pressure, pH 3.0 and 100 °C reaction temperature).

the short chain carboxylic acids are continuously generated and accumulate in the oxidation reaction. As shown in Fig. 7, after 60 min, the short chain carboxylic acids almost completely disappear from the reaction mixture, whereas formic and acetic acids decline more slowly. Therefore, suggesting that the oxidation rate of both formic and acetic acids is the key step for total mineralization of phenol to CO_2 and H_2O. After 120 min reaction, short-chain carboxylic acids were oxidized directly into CO_2 and H_2O. These results are in agreement with the findings reported by Guo and Al-Dahhan [42].

The effectiveness of the oxidation of phenol has also been analysed in terms of TOC removal measured and calculated from intermediates. Fig. 7 (insert) shows the evolution of TOC actual measured and calculated with reaction time; the difference between these two values corresponds to the unidentified intermediates. The measured TOC removal has been depicted together with the calculated TOC corresponding to phenol and the analyzed intermediates; the two curves TOC removal against reaction time can be fitted together.

Influence of the operational parameters and kinetic study for the CWAO of phenol

In order to obtain efficient CWAO of phenol and their kinetic analysis, the influence of the crucial operational parameters such as mass transfer, initial pH, catalyst dosage, initial phenol concentration, reaction temperature and oxygen partial pressure were evaluated. In studying the kinetics of a chemical reaction that is surface-catalysed, it is important to evaluate the relative contributions of mass transfer and true surface reaction. A diffusion-controlled reaction rate will be greatly affected by changes in the degree of agitation. In order to study the dependence of the reaction on the stirring rate on the conversion of phenol, the stirring rate was varied between 200 – 1000 rpm) at 100 °C using 2 g/L catalyst and 1000 mg/L as initial phenol concentration for 150 min reaction time. As shown in Fig. 8, the increase in phenol conversion rate shows a mass transfer regime from 200 to 600 rpm. However, further increase in stirring speed beyond 600 rpm did not increase the phenol conversion rate, which suggests that mass transfer limitation has no effect on the phenol conversion rate over that range. Consequently, all other kinetic study experiments were carried out at 600 rpm to ensure a kinetically controlled regime.

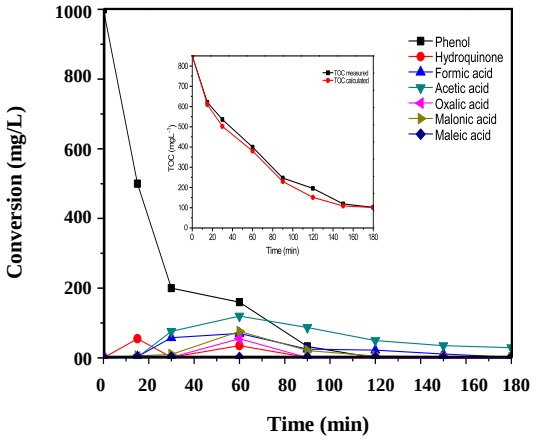

Fig. 7: Evolution of phenol and intermediates in the CWAO reaction of phenol over the Al/Zr-PILC (3:1) (insert shows comparison between calculated and experimental TOC).

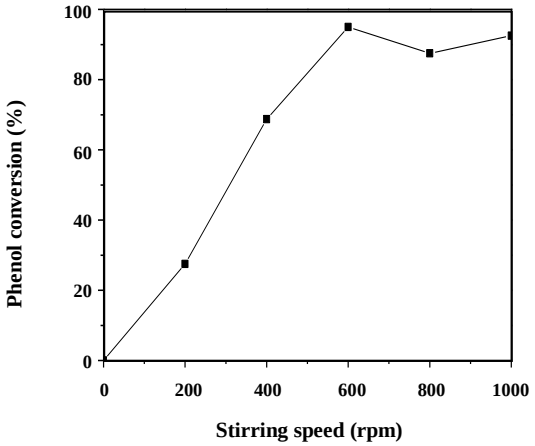

Fig. 8: Effect of mass transfer on the conversion of phenol in aqueous solution. Experimental conditions: phenol, 1000 mg/L; volume, 200 mL; catalyst loading, 2 g/L; reaction time, 150 min; partial oxygen pressure, 10 bar; temperature, 100 °C.

The initial pH of the phenol solution is an important parameter influencing the oxidation of phenol on the CWAO process [35, 89]. The effect of initial solution pH was studied at pH values of 3, 3.5 and 4 as shown in Fig. 9. The conversion of phenol decreases with increasing initial solution pH; the results obtained indicate that optimum pH for maximum phenol conversion in the pH range studied, is pH 3. All reactions for studying the kinetics of the reaction were therefore carried out at pH 3. In view of the fact that CWAO of phenol occurs on the catalyst surface, the process is primarily driven by electrostatic forces. Zeta potential measurements at different pH values provide key information to understanding the interaction and affinity between the catalyst and the phenol solution. As shown in Fig. 2, the point of zero charge for optimum Al/Zr-PILC (3:1) was at pH 3.8. Therefore, the catalyst surface will be positively charged for pH < 3.8, negatively charged for pH > 3.8 and neutral for pH = 3.8, while phenol with pKa of 9.95 is reported to be charged negatively under acidic conditions (studied pH range). Then the conversion of phenol is dependent on the distribution of the species of phenol and the surface charge of Al/Zr-PILC and the existence of cations or anions in the solution. In the studied pH range, phenol is in its non-ionic form; the adsorption onto the catalyst surface is maximized, while there is a minimization of water solubility. The charge attraction between the positively charged Al/Zr-PILC particles and negatively charged phenol molecules increases the affinity of phenol molecules with Al/Zr-PILC particles.

The results of the effect of pH on conversion rate constant were investigated and the results are indicated in the inset of Fig. 8. The experimental data presents good first-order kinetic behaviour. As shown in Fig. 9 (insert), the highest reaction rate constant is obtained at pH 3 where the phenol conversion rate reached 94% within 60 min. However, increase in pH beyond 3 resulted in the decrease of the reaction rate constant values; consequently decrease in the conversion of phenol efficiency (79%). Therefore, the optimal pH of 3 was chosen in this work.

To investigate the effect of the phenol solution concentration on the reaction, it was varied from 500 to 1500 mg/L. As shown in Fig. 10, the phenol conversion decreases with increasing initial concentration of phenol. The decrease in phenol conversion at higher initial phenol concentrations can be as a result of competition for the catalyst active sites by the phenol reactant in solution as well as an increase in mass transfer limitation of phenol and consequently a decrease in the rate at which phenol molecules adsorb on the catalyst surface from solution. The results are in consistent with those obtained by other researchers [4, 42-44], indicating that the catalytic activity of phenol decreases with increasing initial phenol concentration. The effect of initial phenol concentration on apparent kinetic rate constant is shown in the inset of Fig. 10. The results display a good linear relationship of

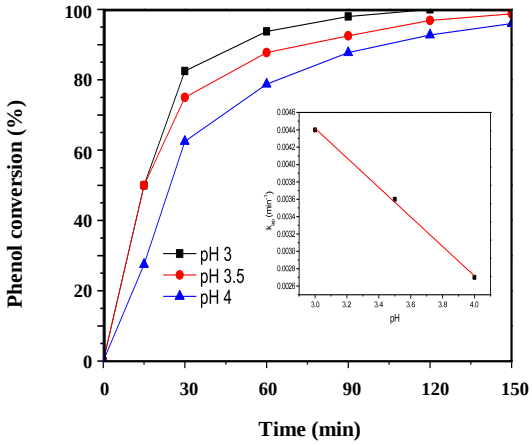

Fig. 9: Effect of initial pH on conversion of phenol in aqueous solution (a) and the corresponding effect on rate constant (b). Experimental conditions: phenol, 1000 mg/L; volume, 200 mL; catalyst loading, 2 g/L; reaction time, 150 min; partial oxygen pressure, 10 bar; temperature, 100 °C.

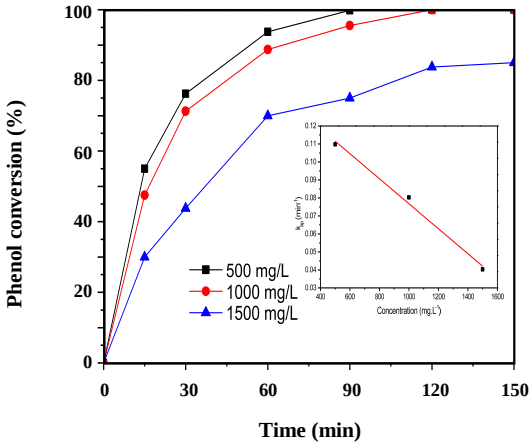

Fig. 10: Effect of initial concentration of phenol in aqueous solution (a) and the corresponding effect on rate constant (b). Experimental conditions: volume, 200 mL; catalyst loading, 2 g/L; pH, 3.0; reaction time, 150 min; partial oxygen pressure, 10 bar; temperature 100 °C.

apparent rate constant as a function of initial phenol concentration. The phenol conversion was fitted using first-order kinetic, as confirmed by the observed straight line. The inset of Fig. 10 shows that the apparent kinetic rate constant decreased with increase of initial phenol concentration. Accordingly, there is a slight increase in apparent kinetic rate constant from 0.0803 min^{-1} to 0.1098 min^{-1} over the initial phenol concentration from 1000 to 500 mg/L. As a result, 1000 mg/L was chosen as the optimal initial phenol concentration in this study.

The optimum catalyst dosage in the reactor was investigated by varying the catalyst mass for the reaction between 1 – 3 g/L of phenol solution maintaining the other parameters constant. Fig. 11 show the dependence of the phenol conversion as a function of catalyst amount. An increase in phenol conversion is observed with an increasing catalyst amount from 1 to 2 g/L. However, a further increase to 3 g/L results in a decrease in the phenol conversion. The decrease in conversion with an increase in catalyst amount can be attributed to a decrease in catalyst active sites as a result of agglomeration of the excess catalyst particles in the slurry. A free-radical chain reaction for CWAO of phenol has been proposed by some researchers [45-47]. In this mechanism the competition between free radical formation and free radical termination is expected to take place and both rates increase with an increase in catalyst amount. The results indicate that the free radical formation rate is higher at a lower catalyst loading, while at excessive higher catalyst loading, free radical termination rate dominates the reaction. Therefore, 2 g/L catalyst dosage can be considered optimum for obtaining maximum phenol conversion in the studied range and subsequent experiments were performed at 2 g/L. The effect of catalyst dosage on the apparent kinetic rate constant of phenol is shown in the inset of Fig. 9. The linear trend of apparent kinetic rate constant as function of catalyst loading shown in Fig. 9 (inset) indicates that the reaction obeys first-order kinetics. The apparent kinetic rate constant increased from 0.0127 min^{-1} to 0.0432 min^{-1} with the increase in catalyst mass from 1 to 2 g/L and then decreased to 0.0297 min^{-1} with a catalyst mass of 3 g/L. Therefore, the highest apparent kinetic rate constant was observed at catalyst loading of 2 g/L with phenol conversion rate of 94% within 120 min.

In order to investigate the effect of temperature on the CWAO of phenol in aqueous solution catalysed by the Al/Zr pillared clay catalyst, the experiments with different temperatures (80 °C, 100 °C and 120 °C) were set up. Fig. 12 shows that the phenol conversion increases with temperature. It is observed that at lower temperatures, the required reaction time was longer than at high temperature. However, at longer reaction times, the difference in phenol conversions at 100 °C and 120 °C are not significantly different. The reaction temperature of 100 °C was considered the optimal

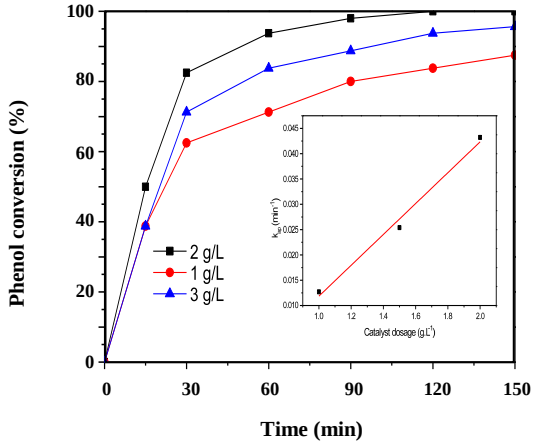

Fig. 11: Effect of catalyst dosage on conversion of phenol in aqueous solution (a) and the corresponding effect on rate constant (b). Experimental conditions: phenol, 1000 mg/L; volume, 200 mL; pH, 3.0; reaction time, 150 min; partial oxygen pressure, 10 bar; temperature, 100 °C.

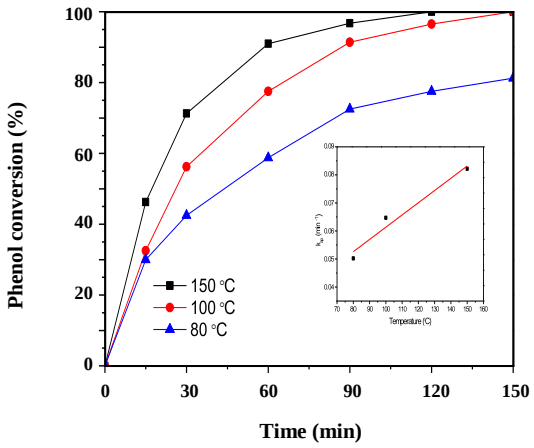

Fig. 12: Effect of reaction temperature on conversion of phenol in aqueous solution (a) and the corresponding effect on rate constant (b). Experimental conditions: phenol, 1000 mg/L; volume, 200 mL; pH, 3.0; reaction time, 180 min; partial oxygen pressure, 10 bar; catalyst loading, 2 g/L.

reaction temperature in the study. This trend suggests that the reaction temperature strongly affects the CWAO of phenol and can be ascribed to intermediate compounds such as aromatics and organic acids which are reported by other researches to be produced during the reaction [4, 46, 47]. When all these organic compounds are removed, the remaining aliphatic compounds (mainly carboxylic acids) become resistant to oxidation or occur at low rate, even at high temperatures, and the overall oxidation process decreases. In comparison with actual industrial CWAO operation temperature between 200 to 325 °C, the lower reaction temperature required by Al/Zr-pillared clay catalyst would possibly result in high energy cost savings. The influence of reaction temperature on the apparent kinetic reaction rate constant was investigated as shown in the inset of Fig. 12. A linear relation between the apparent rate constant and the reaction temperature is observed and it is evident that the apparent rate constant of phenol conversion increases with reaction temperature.

The effect of oxygen partial pressure on the phenol conversion rate was studied by varying different pressures from 5 to 15 bar and the results are presented in Fig. 13. There is an increase in the phenol conversion with increasing oxygen partial pressure. The phenol conversion reached 74% at 5 bar of oxygen partial pressure while complete removal of phenol was reached at 10 and 15 bar after 120 min reaction time. This is as a result of the fact that the concentration and solubility of the oxygen gas increase with increasing pressure resulting in a faster phenol oxidation rate. This effect might be correlated to the availability of liquid oxygen to the active site of the pillared clay catalysts. According to the Henry's law, the partial pressure of oxygen in the gas phase is directly proportional to the oxygen dissolved in the liquid phase. However, an increase in the oxygen partial pressure from 10 to 15 bar does not result in a significant increase in the phenol conversion. And consequently, the oxygen partial pressure of 10 bar was considered as the optimum value in this study. The effect of oxygen partial pressure on the kinetic reaction rate constant of phenol oxidation was investigated and the results are shown in the inset of Fig. 13. There is a linear relationship of apparent rate constant as function of oxygen partial pressure confirming that the experimental data obtained can be described by the first-order kinetic model. An increase in the kinetic reaction rate constant with the oxygen partial pressure was observed.

Activation Energy

In order to determine the apparent activation energy, the experiments were carried out under the predetermined optimal experimental conditions at the three different temperatures. The Arrhenius plot obtained is shown in Fig. 14. The plot presents a good linear relationship (R^2 = 0.9875) between ln k_{ap} and 1/T indicating that the experimental data follow the Arrhenius-type behaviour.

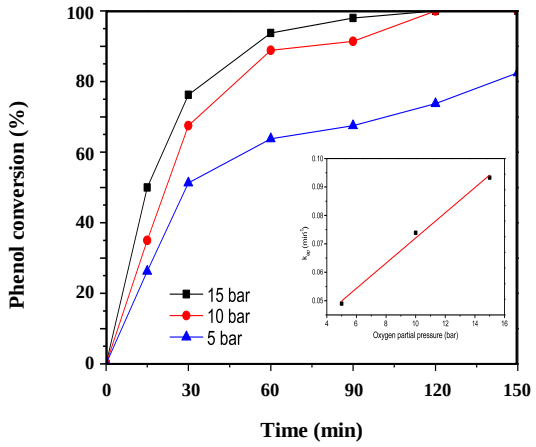

Fig. 13: Effect of oxygen partial pressure on conversion of phenol in aqueous solution (a) and the corresponding effect on rate constant (b). Experimental conditions: phenol, 1000 mg/L; volume, 200 mL; pH, 3.0; reaction time, 180 min; temperature, 100 °C; catalyst loading, 2 g/L.

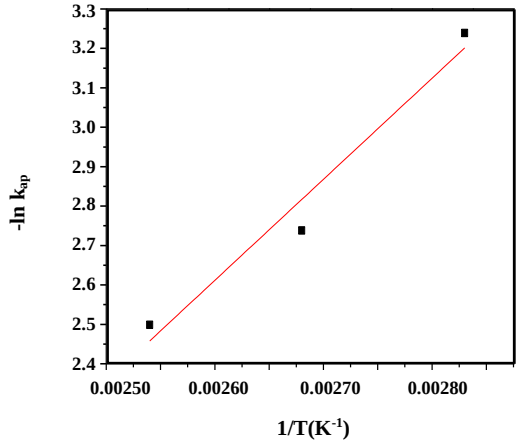

Fig. 14: Arrhenius plot for determining E_a (apparent activation energy) and k_o (pre-exponential factor) for the CWAO of phenol in aqueous solution. (1000 mg/L phenol; 200 mL volume; pH 3; 100 °C reaction temperature; catalyst loading, 2 g/L).

The slope and intercept of the straight line were used to determine apparent activation energy (E_a) and pre-exponential factor (k_0), respectively. To the best of our knowledge, there is no study published in the open literature in which these kinetic parameters are reported on the CWAO of phenol using Al/Zr-pillared clay catalysts. However, the kinetics of phenol oxidation using Al/Fe-pillared extrudates has been reported with an apparent activation energy of 53.306 kJ/mol [4]. It should be noted that such kinetic approach does not correspond to actual intrinsic kinetics since extrudates were used and not powder catalysts as in our study. The observed apparent activation energy and pre-exponential factor of phenol oxidation were found to be 21.306 kJ/mol and 0.512 min^{-1}, which were lower than 24.62 to 176 kJ/mol values obtained in other studies using different catalyst systems [2, 12, 14, 48-51]. These results indicate that the CWAO of phenol using Al/Zr pillared clay catalyst requires a relatively low activation energy compared to other systems studied; and can be easily achieved.

CONCLUSIONS

The natural bentonite clay was successfully pillared with single and mixed metal oxides of Al and Zr using ultrasonic treatment. Its catalytic performance was evaluated in the CWAO of phenol in an aqueous solution by semi-batch reactor. XRD analysis confirmed the successful pillaring of bentonite clay. The incorporation of Al^{3+} and Zr^{4+} species into pillared bentonite clay was confirmed by EDX. The results of characterization of synthesized catalysts indicated that the basal spacing, BET surface area, pore volume, surface acidity and thermal stability of mixed Al/Zr-PILC was significantly higher than single Al-PILC, Zr-PILC and natural bentonite clay.

Furthermore, the study indicates the potential of pillared bentonite clay catalysts for the removal of phenol from aqueous solutions under mild reaction conditions of the CWAO process. And the Al/Zr-PILC composite with metal Al:Zr ratio of 3:1 was found to be very active among different pillared catalysts and the complete removal of phenol from solution was achieved within 120 min. The CWAO process was affected by reaction parameters, such as initial pH, catalyst loading, initial phenol concentration reaction temperature and oxygen partial pressure. The optimal reaction parameters were achieved at initial pH 3, catalyst loading of 2 g/L, phenol concentration of 1000 mg/L at reaction temperature of 100 °C and 10 bar oxygen partial pressure. The experimental results indicate that the phenol oxidation can be described by first-order kinetics, with apparent activation energy of 21.306 kJ mol^{-1}. The Al/Zr-PILC composite catalyst exhibited good results for removal of phenol in aqueous solution at mild condition by CWAO and has the potential to substitute the expensive noble metal catalysts.

Acknowledgments

The authors are grateful to the National Research Foundation (NRF)/ Department of Science and Technology (DST) of South Africa (Project code. 96719) and Mineral Science Council of South Africa (Mintek) (Project code. ADR 31803) for financial support.

Received : Jun. 23, 2018 ; Accepted : Sep. 15, 2018

REFERENCES

[1] Baloyi J., Ntho T., Moma J., Synthesis and Application of Pillared Clay Heterogeneous Catalysts for Wastewater Treatment: A Review, *RSC Advances*, **8**: 5197-5211 (2018).

[2] Abid M.F., Alwan G.M., Abdul-Ridha L.A., Study on Catalytic Wet Air Oxidation Process for Phenol Degradation in Synthetic Wastewater Using Trickle Bed Reactor, *Arabian Journal for Science and Engineering*, **41**: 2659-2670 (2016).

[3] Eftaxias A., Font J., Fortuny A., Fabregat A.,Stüber F., Kinetics of Phenol Oxidation in a Trickle Bed Reactor over Active Carbon Catalyst, *Journal of Chemical Technology and Biotechnology*, **80**: 677-687 (2005).

[4] Guo J., Catalytic Wet Oxidation over Pillared Clay Catalyst in Packed-Bed Reactors: Experiments and Modeling, DSc dissertation, (2005), Washington University, Missouri, USA.

[5] Arena F., Italiano C., Spadaro L., Efficiency and Reactivity Pattern of Ceria-Based Noble Metal and Transition Metal-Oxide Catalysts in the Wet Air Oxidation of Phenol, *Applied Catalysis B: Environmental*, **115**: 336-345(2012).

[6] Tomul F., Effect of Ultrasound on the Structural and Textural Properties of Copper-Impregnated Cerium-Modified Zirconium-Pillared Bentonite, *Applied Surface Science*, **258**: 1836-1848(2011).

[7] Sassi H., Lafaye G., Amor H.B., Gannouni A., Jeday M.R., Barbier J., Wastewater Treatment by Catalytic Wet Air Oxidation Process over Al-Fe Pillared Clays Synthesized Using Microwave Irradiation, *Frontiers of Environmental Science & Engineering*, **12**, 2 (2018).
https://doi.org/10.1007/s11783-017-0971-1.

[8] Mnasri-Ghnimi S., Frini-Srasra N., Promoting Effect of Cerium on the Characteristic and Catalytic Activity of Al, Zr, and Al–Zr Pillared Clay, *Applied Clay Science*, **88**: 214-220 (2014).

[9] Ma C., Wen Y., Yue Q., Li A., Fu J., Zhang N., Gai H., Zheng J., Chen B.H., Oxygen-Vacancy-Promoted Catalytic Wet Air Oxidation of Phenol from MnOx–CeO_2, *RSC Advances*, **7**: 27079-27088 (2017).

[10] Fortuny A., Bengoa C., Font J., Fabregat A., Bimetallic Catalysts for Continuous Catalytic Wet Air Oxidation of Phenol, *Journal of Hazardous Materials*, **64**: 181-193 (1999).

[11] Eftaxias A., "Catalytic Wet Air Oxidation of Phenol in a Trickle Bed Reactor: Kinteics and Reactor Modelling", Universitat Rovira i Virgili, (2002).

[12] Pintar A., Levec J., Catalytic Oxidation of Organics in Aqueous Solutions: I. Kinetics of Phenol Oxidation, *Journal of Catalysis*, **135**: 345-357 (1992).

[13] Fortuny A., Bengoa C., Font J., Castells F., Fabregat A., Water pollution Abatement by Catalytic Wet Air Oxidation in a Trickle Bed Reactor, *Catalysis Today*, **53**: 107-114(1999).

[14] Safaa M., Catalytic Wet Air Oxidation of Phenolic Compounds in Wastewater in a Trickle Bed Reactor at High Pressure, MSc thesis, University of Tikrit, (2009).

[15] Quintanilla A., Casas J.A., Rodriguez J.J., Kreutzer M.T., Kapteijn F., Moulijn J.A., Kinetics of the Wet Oxidation of Phenol over an Fe/Activated Carbon Catalyst, *International Journal of Chemical Reactor Engineering*, **5 (1)** (2007).
https://doi.org/10.2202/1542-6580.1555.

[16] Quintanilla A., Casas J.A., Rodriguez J.J., Catalytic Wet Air Oxidation of Phenol with Modified Activated Carbons and Fe/Activated Carbon Catalysts, *Applied Catalysis B: Environmental*, **76**: 135-145 (2007).

[17] Tomul F., Balci S., Characterization of Al, Cr-Pillared Clays and CO Oxidation, *Applied Clay Science*, **43 (1)**: 13-20 (2009).

[18] Grim R.E., "Clay Mineralogy". 2nd ed. McGraw-Hill Book Company, New York, (1968) 185-224.

[19] Schwieger W., Lagaly G., Auerbach S.M., Carrado K.A., Dutta P.K., Handbook of layered Materials, in, Marcel Dekker, Inc., New York,(2004).

[20] Canizares P., Valverde J.L., Kou M.R.S., Molina C.B., Synthesis and Characterization of PILCs with Single and Mixed Oxide Pillars Prepared from Two Different Bentonites, *A Comparative Study, Microporous and Mesoporous Materials*, **29**: 267-281 (1999).

[21] Awate S.V., Waghmode S.B., Agashe M.S., Synthesis, Characterization and Catalytic Evaluation of Zirconia-Pillared Montmorillonite for Linear Alkylation of Benzene, *Catalysis Communications*, **5**: 407-411(2004).

[22] Jung H., Paek S.-M., Yoon J.-B., Choy J.-H., Zr K-Edge XAS Study on ZrO_2-Pillared Aluminosilicate, *Journal of Porous Materials*, **14**: 369-377(2007).

[23] Mnasri S., Hamdi N., Frini-Srasra N., Srasra E., Acid–Base Properties of Pillared Interlayered Clays with Single and Mixed Zr–Al Oxide Pillars Prepared from Tunisian-Interstratified Illite–Smectite, *Arabian Journal of Chemistry*, (2014).

[24] Zhang H., Liang X., Yang C., Niu C., Wang J., Su X., Nano γ-Fe_2O_3/Bentonite Magnetic Composites: Synthesis, Characterization and Application as Adsorbents, *Journal of Alloys and Compounds*, **688**: 1019-1027(2016).

[25] Rathnayake S.I., Martens W.N., Xi Y., Frost R.L., Ayoko G.A., Remediation of Cr (VI) by Inorganic-Organic Clay, *Journal of Colloid and Interface Science*, **490**: 163-173(2017).

[26] Madejová J., FTIR Techniques in Clay Mineral Studies, Vibrational Spectroscopy, **31**: 1-10(2003).

[27] Kumararaja P., Manjaiah K.M., Datta S.C., Sarkar B., Remediation of Metal Contaminated Soil by Aluminium Pillared Bentonite: Synthesis, Characterisation, Equilibrium Study and Plant Growth Experiment, *Applied Clay Science*, **137**: 115-122 (2017).

[28] Basoglu F.T., Balci S., Catalytic Properties and Activity of Copper and Silver Containing Al-Pillared Bentonite for CO Oxidation, *Journal of Molecular Structure*, **1106**: 382-389(2016).

[29] Wu L.M., Tong D.S., Zhao L.Z., Yu W.H., Zhou C.H., Wang H., Fourier Transform Infrared Spectroscopy Analysis for Hydrothermal Transformation of Microcrystalline Cellulose on Montmorillonite, *Applied Clay Science*, **95**: 74-82(2014).

[30] Acemana S., Lahav N., Yariv S., A Thermo-FTIR-Spectroscopy Analysis of Al-Pillared Smectites Differing in Source of Charge, in KBr Disks, *Thermochimica Acta*, **340**: 349-366(1999).

[31] Ye W., Zhao B., Gao H., Huang J., Zhang X., Preparation of Highly Efficient and Stable Fe, Zn, Al-Pillared Montmorillonite as Heterogeneous Catalyst for Catalytic Wet Peroxide Oxidation of Orange II, *Journal of Porous Materials*, **23**: 301-310 (2016).

[32] Lefrancois M., Malbois G., The Nature of the Acidic Sites on Mordenite, *Journal of Catalysis*, **20**: 350-358 (1971).

[33] Kojima M., Rautenbach M.W., O'Connor C.T., Acidity Characterization of Ion-Exchanged Mordenite, *Journal of Catalysis*, **112**: 495-504 (1988).

[34] Loveless B.T., Gyanani A., Muggli D.S., Discrepancy between TPD-and FTIR-Based Measurements of Brønsted and Lewis Acidity for Sulfated Zirconia, *Applied Catalysis B: Environmental*, **84**: 591-597 (2008).

[35] Fatimah I., Preparation of ZrO2/Al_2O_3-Montmorillonite Composite as Catalyst for Phenol Hydroxylation, *Journal of Advanced Research*, **5**: 663-670 (2014).

[36] Fetter G., Heredia G., Velázquez L.A., Maubert A.M., Bosch P., Synthesis of Sluminum-Pillared Montmorillonites Using Highly Concentrated clay Suspensions, *Applied Catalysis A: General*, **162**: 41-45 (1997).

[37] Fetter G., Heredia G., Maubert A.M., Bosch P., Synthesis of Al-Intercalated Montmorillonites Using Microwave Irradiation, *Journal of Materials Chemistry*, **6**: 1857-1858 (1996).

[38] Katdare S.P., Ramaswamy V., Ramaswamy A.V., Factors Affecting the Preparation of Alumina Pillared Montmorillonite Employing Ultrasonics, *Microporous and Mesoporous Materials*, **37**: 329-336 (2000).

[39] Santos A., Yustos P., Quintanilla A., Rodrıguez S., Garcıa-Ochoa F., Route of the Catalytic Oxidation of Phenol in Aqueous Phase, *Applied Catalysis B: Environmental*, **39**: 97-113(2002).

[40] Yang G., Chen H., Qin H., Zhang X., Feng Y., Effect of Nitrogen Doping on the Catalytic Activity of Activated Carbon and Distribution of Oxidation Products in Catalytic Wet Oxidation of Phenol, *The Canadian Journal of Chemical Engineering*, **95**: 1518-1525 (2017).

[41] Yang S., Li X., Zhu W., Wang J., Descorme C., Catalytic Activity, Stability and Structure of Multi-Walled Carbon Nanotubes in the Wet Air Oxidation of Phenol, *Carbon*, **46**: 445-452 (2008).

[42] Guo J., Al-Dahhan M., Catalytic Wet Oxidation of Phenol by Hydrogen Peroxide over Pillared Clay Catalyst, *Industrial & Engineering Chemistry Research*, **42**: 2450-2460 (2003).

[43] Yadav A.,. Teja A.K, Verma N., Removal of Phenol from Water by Catalytic wet Air Oxidation Using Carbon Bead–Supported Iron Nanoparticle–Containing Carbon Nanofibers in an Especially Configured Reactor, *Journal of Environmental Chemical Engineering*, **4**: 1504-1513 (2016).

[44] Wu Q., Hu X., Yue P.-l., Kinetics Study on Catalytic Wet Air Oxidation of Phenol, *Chemical Engineering Scienc*e, **58**: 923-928(2003).

[45] Lin S.S., Chang D.J., Wang C.-H., Chen C.C., Catalytic Wet Air Oxidation of Phenol by CeO_2 Catalyst—Effect of Reaction Conditions, *Water Research*, **37**: 793-800(2003).

[46] Arena F., Italiano C., Raneri A., Saja C., Mechanistic and Kinetic Insights into the Wet Air Oxidation of Phenol with Oxygen (CWAO) by Homogeneous and Heterogeneous Transition-Metal Catalysts, *Applied Catalysis B: Environmental*, **99**: 321-328 (2010).

[47] Chang L., Chen I.P., Lin S.-S., An Assessment of the Suitable Operating Conditions for the CeO_2/γ-Al_2O_3 Catalyzed Wet Air Oxidation of Phenol, *Chemosphere*, **58**: 485-492(2005).

[48] Pintar A., Levec J., Catalytic Liquid-Phase Oxidation of Refractory Organics in Waste Water, *Chemical Engineering Science*, **47**: 2395-2400 (1992).

[49] Santos A., Yustos P., Quintanilla A., Garcia-Ochoa F., Kinetic model of Wet Oxidation of Phenol at Basic pH Using a Copper Catalyst, *Chemical Engineering Science*, **60**: 4866-4878 (2005).

[50] Akyurtlu J.F., Akyurtlu A., Kovenklioglu S., Catalytic Oxidation of Phenol in Aqueous Solutions, *Catalysis Today*, **40**: 343-352(1998).

[51] Stüber F., Polaert I., Delmas H., Font J., Fortuny A., Fabregat A., Catalytic Wet Air Oxidation of Phenol Using Active Carbon: Performance of Discontinuous and Continuous Reactors, *Journal of Chemical Technology and Biotechnology*, **76**: 743-751(2001).

Supplementary Material

Table 1S: Chemical analysis of natural and pillared bentonite clay.

Sample	Al/Zr ratio	Na (%)	Mg (%)	Al (%)	Si (%)	K (%)	Ca (%)	Fe (%)	Zr (%)
Na-Bt	-	3.73	3.29	15.31	65.09	2.39	1.09	9.10	0.00
Al-PILC	-	0.96	1.24	31.98	59.14	1.82	0.27	4.55	0.00
Zr-PILC	-	0.88	1.33	11.74	41.83	1.57	0.11	4.35	38.19
Al/Zr-PILC	1:3	0.19	1.88	18.06	54.98	1.31	0.09	1.51	21.98
Al/Zr-PILC	1:1	0.98	1.25	20.27	56.38	1.45	0.76	1.31	17.60
Al/Zr-PILC	3:1	0.26	1.29	23.65	54.47	1.41	0.04	1.61	17.31
Al/Zr-PILC	6:1	0.58	1.59	25.89	52.64	1.36	0.57	0.99	16.38

Table 2S: Surface properties of prepared catalysts and raw bentonite clay.

Sample	S1BET (m2/g)	V2pore (cm3/g)	V3mic (cm3/g)	d4pore (nm)
Na-Bt	61	0.11	0.089	10.1
Zr-PILC	150	0.33	0.106	8.5
Al-PILC	147	0.32	0.099	8.2
Al/Zr-PILC(1:3)	206	0.35	0.110	7.2
Al/Zr-PILC(1:1)	210	0.36	0.113	7.6
Al/Zr-PILC(3:1)	230	0.38	0.115	7.1
Al/Zr-PILC(6:1)	182	0.34	0.108	7.8

1 Specific surface area (SBET); 2 Total pore volume at p/p0 ~ 0, 99; 3 Micropore volume; 4 Pore diameter.

Table 3S: XRD analyses data for the natural and pillared bentonite clays.

Sample	Al/Zr ratios	2θ (degree)	d001 (nm)
Na-Bt	Host	8.88	1.56
Al-PILC	-	7.30	1.72
Zr-PILC	-	7.22	1.79
Al/Zr-PILC	1:3	7.19	1.81
Al/Zr-PILC	1:1	7.14	1.88
Al/Zr-PILC	3:1	6.84	1.92
Al/Zr-PILC	6:1	6.88	1.78